Solid-State Tautomerism in 2-Carboxyindan-1,3-dione

7 AUTHORS, INCLUDING:

Venelin Enchev
Bulgarian Academy of Sciences
103 PUBLICATIONS   **808** CITATIONS

SEE PROFILE

Silvia Angelova
Bulgarian Academy of Sciences
43 PUBLICATIONS   **160** CITATIONS

SEE PROFILE

Marin Rogozherov
Bulgarian Academy of Sciences
19 PUBLICATIONS   **108** CITATIONS

SEE PROFILE

Iwona Wawer
Medical University of Warsaw
157 PUBLICATIONS   **1,224** CITATIONS

SEE PROFILE

Solid-State Tautomerism in 2-Carboxyindan-1,3-dione

Venelin Enchev,*,[†] Silvia Angelova,[†] Marin Rogojerov,[†] Valentin Monev,[†] Iwona Wawer,[‡] Michał Tkaczyk,[‡] and Kalina Kostova[†]

[†]Institute of Organic Chemistry, Bulgarian Academy of Sciences, 1113 Sofia, Bulgaria

[‡]Faculty of Pharmacy, Medical University of Warsaw, Banacha 1, 02097 Warsaw, Poland

S *Supporting Information*

ABSTRACT: The structure of 2-carboxyindan-1,3-dione was investigated using a combination of quantum-chemical calculations and solid-state NMR and IR spectroscopy. Due to poor solubility of the compound in different solvents, no single crystals could be obtained. Two dimeric structures formed from the tautomers of 2-carboxyindan-1,3-dione are likely to coexist in the solid state. The dimers interconvert via intramolecular proton transfer in one of the tautomeric forms constituting the dimers. The energy barrier of the intramolecular proton transfer reaction is calculated as 5.82 kcal mol^{-1} at the MP2/6-31++G level of theory.
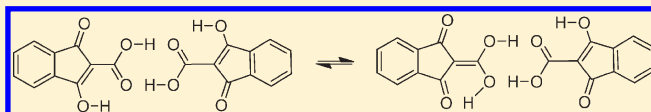
1. INTRODUCTION

Equilibria connected with proton transfer are responsible for important properties like photo- and thermochromism of compounds containing internal hydrogen bonds. Among the great number of photo- and thermochromic compounds investigated,[1] few have been found to be photochromic[2] or thermochromic[3–5] in the crystalline phase. Applications as switches and sensors can be foreseen.[2e] Studying the solid-state tautomerism in Schiff bases derived from 3-hydroxysalicylaldehyde, Pizzala et al.[6] reported the presence of OH- and NH-forms in fast equilibrium with a low activation barrier. Ultrafast intramolecular proton transfer in solid N,N′-diphenyl-6-aminofulvene-1-aldimine was detected by Limbach et al.[7] Recently, Elguero et al.[8] showed how tautomers linked by two hydrogen bonds display a very fast intermolecular double proton transfer in the solid state. We also found[9] ultrafast intramolecular proton transfer in 2-(hydroxyaminomethylidene)-indan-1,3-dione in solid state and suggest that because of this the compound sinters from 180 to 220 °C. The above-mentioned compound is related to 2-carboxyindan-1,3-dione.

2-Carboxyindan-1,3-dione was obtained 130 years ago,[10,11] but for a long time the structure of the compound was not elucidated.[11,12] It has been synthesized by Perkin condensation of phthalic anhydride with acetic anhydride and potassium acetate followed by isomerization of the phthalidene acetic acid with sodium methoxide and subsequent hydrolysis of the sodium salt with HCl.

2-Carboxyindan-1,3-dione exhibits interesting tautomeric behavior. The compound itself is a crystalline powder of ochre color. It is insoluble in nonpolar solvents but is soluble in dimethylformamide and dimethylsulfoxide with a red-brown color. The solubility in tetrahydrofuran, acetone, methanol, and water is low. The initial yellowish suspension of the substance in these solvents turns within ca. 30 min to a red-brown solution. Recently

we reported that most probably the red-brown color of the solution is an indication of the formation of the anionic form or a mixture of anion and dianion.[13]

The structure of the compound in the solid state is unclear. 2-Carboxyindan-1,3-dione does not form single crystals, and X-ray analysis cannot be performed.

An interesting question arises as to if the tautomers of 2-carboxyindan-1,3-dione can form various hydrogen-bonded dimers and what are their relative stabilities. Further, they could exist as a mixture of dimers in equilibrium. Intramolecular proton transfer in the constituents is also possible. In principle, this complex equilibrium could be studied by NMR if the proton exchange is slow enough on the NMR time scale.

The goal of the present work is to elucidate the structure of 2-carboxyindan-1,3-dione in the solid state and, if the compound exists in homo- or heterodimeric form, whether intramolecular proton transfer is possible. It would not be surprising, since cases in which the same crystal contains two tautomers forming hydrogen-bonded dimers have already been reported.[14]

2. COMPUTATIONAL AND EXPERIMENTAL DETAILS

2.1. Computational Details. The geometries of the possible tautomers and rotamers of 2-carboxyindan-1,3-dione and the possible dimeric structures were located at HF and MP2 levels using the Pople basis sets 6-31G(d,p), 6-31+G(d,p), and 6-31++G. Full geometry optimization of the structures investigated was performed without symmetry constraints. The default gradient convergence threshold 1×10^{-4} hartree ·bohr^{-1} was used. The local minima and transition states were verified by establishing that the Hessians have zero and one

negative eigenvalues, respectively. To estimate the enthalpies at 0 K (ΔH_0), the ZPE corrections were added to the calculated total energies. The values of Gibbs free energies (ΔG) and activation barriers ($\Delta G^{\#}$) were calculated for a temperature of 298.15 K. The classical rate constant at 298.15 K was calculated using the Eyring equation, $k = (k_B T/h)e^{-\Delta G^{\#}/RT}$, where k_B and h are the Boltzmann and Planck constants, respectively.

Starting from the transition state, the reaction path was generated as the steepest descent path in mass-scaled coordinates (intrinsic reaction coordinate, IRC) at the MP2/6-31++G level using the Gonzalez–Schlegel algorithm,[15] employing a step size of 0.05 bohr (1 bohr corresponds to 0.53 Å). On both branches of the reaction coordinate, 30 steps were performed.

Single-point calculations at the CCSD(T)[16] level using MP2 geometry were also performed for all tautomers and rotamers of 2-carboxyindan-1,3-dione. The values of enthalpies and Gibbs free energies at the CCSD(T) level were obtained using the MP2 calculated ZPE and entropy corrections. The calculations were carried out using the GAMESS (US) quantum chemistry package.[17]

Additional calculations were done using the computational chemistry program Firefly[18] at DFT (X3LYP hybrid functional[19]) and MP2 levels of theory, using Dunning's triple-ζ cc-pVTZ basis set and a truncated version cc-pVTZ- (minus the f shell on heavy atoms and the d shell on the hydrogen atom).[20] Symmetry was used whenever possible to increase efficiency and aid the interpretation of results. Delocalized internal coordinates were automatically generated and used to speed geometry optimizations but also to make certain that symmetry was not a preconceived artifact (dlc's are not symmetry-preserving). Extra high precision (1×10^{-6} hartree·bohr^{-1} gradient convergence threshold) was specified throughout the calculations to avoid imaginary frequencies at the geometry minima.

The theoretically predicted O–H and C=O frequencies were scaled by different factors c determined by means of a least-squares procedure proposed in ref 21

$$c = [\sum_i^N \nu_i^{theor} \cdot \nu_i^{exp}]/[\sum_i^N \nu_i^{theor}]^2$$

where ν_i^{theor} and ν_i^{exp} are calculated and experimental frequencies, respectively, while N is the number of the selected frequency modes for each type of vibration. A similar approach has been applied by Andersson and Uvdal.[22]

The NMR chemical shieldings of selected tautomeric forms and dimers of 2-carboxyindan-1,3-dione were calculated at the OLYP/6-311+G(d,p) level using the GIAO approach[23] and MP2/6-31++G optimized geometry. In order to compare to the experimental data, the calculated absolute shieldings were transformed to chemical shifts using the reference compound tetramethylsilane, Si(CH$_3$)$_4$, for carbon: $\delta = \delta_{calc}(ref) - \delta_{calc}$. Both $\delta_{calc}(ref)$ and δ_{calc} were evaluated at the same computational level. All NMR calculations were carried out using Gaussian 03.[24]

2.2. Experimental Section. The synthesis of the title compound is described in our previous paper.[13]

The solid-state ^{13}C cross-polarization (CP) magic angle spinning (MAS) spectrum was recorded on a Bruker DRX-400 spectrometer at 100.61 MHz. The powder sample was spun at 10 kHz in a 4 mm ZrO$_2$ rotor (contact time of 2 ms, repetition time of 6s), and 600 scans were accumulated. ^{13}C chemical shifts were calibrated indirectly through the glycine CO signal recorded at 176.0 ppm, relative to TMS.
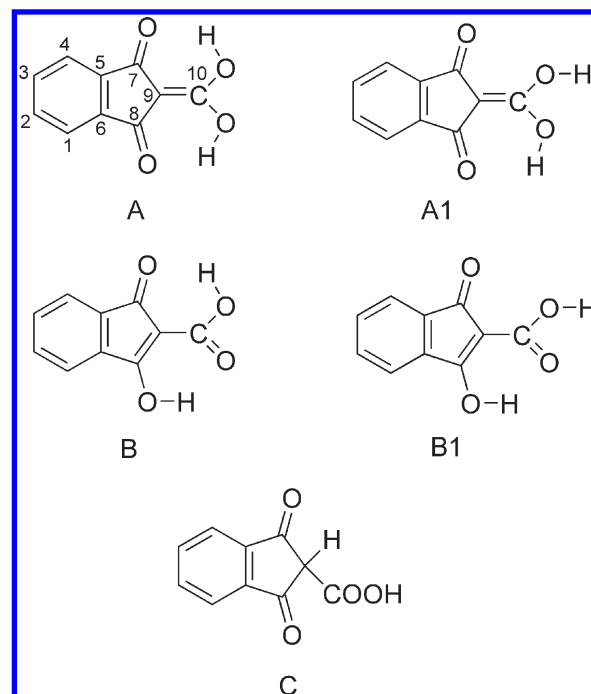
Figure 1. Tautomers (**A**–**C**) and rotamers (**A1**, **B1**) of 2-carboxyindan-1,3-dione.

The infrared spectrum of the crystalline powder was recorded on an FTIR spectrometer Bruker Tensor 27 in the 4000–550 cm^{-1} spectral region with resolution of 2 cm^{-1} using the ATR appliance Pike Miracle with ZnSe Crystal Plate. The far-IR spectrum was recorded on a FTIR spectrometer Bruker IFS 113v in the 480–100 cm^{-1} spectral region with resolution of 2 cm^{-1} by the use of the PE powder technique.

3. RESULTS AND DISCUSSION

3.1. Tautomerism. The geometries of the possible tautomeric forms of 2-carboxyindan-1,3-dione (**A**–**C**) and their rotamers (**A1** and **B1**) (Figure 1) were optimized at the MP2 level using 6-31G(d,p), 6-31+G(d,p), and 6-31++G basis sets. To obtain accurate energies, additional single-point calculations at the CCSD(T) level of theory using the same basis sets were performed. The relative energies of the tautomers and rotamers (isolated molecules) are between 0.15 and 12.3 kcal mol^{-1}, depending on the level of theory (Table 1). The calculations at the MP2 and CCSD(T) level using 6-31++G and 6-31+G(d,p) basis sets predict **C** as the most stable tautomer. However, the presence of tautomer **C** in the solid state is excluded by the experimental ^{13}C NMR spectra because the signal for the C9 atom should be ca. 50–60 ppm, but such a peak is not observed in the spectrum (Figure 2).

3.2. Dimerization. Hydrogen bonding is the main driving force in dimer formation in the case of most compounds involved in tautomerism. As is well established, the hydrogen bond can serve to strongly stabilize the structure. Similar to other organic acids,[25] it could be suggested that 2-carboxyindan-1,3-dione forms dimers in the solid state. Rotamer **B1** is comparable in energy to tautomer **B**, but this form has the ability for hydrogen-bonded dimer formation due to the OH group rotation. Three dimeric structures from the rotamers of tautomers **A** and **B** are possible—**B1B1**, **A1B1**, and **A1A1** (Figure 3). Their relative

enthalpies at 0 K and free energies at 298 K are listed in Table 2. The relative energies are dependent on the basis set. The ab initio and DFT calculations at all computational levels predict dimer **B1B1** to be most stable; next in energy is the "mixed" dimer **A1B1**. Dimer **A1A1** is high in energy.

The presented acid dimers are an example of a system containing four hydrogen bonds—two intermolecular and two intramolecular. These two types of hydrogen bonds are linked by a common oxygen atom which suggests that they may interact.

Table 1. Calculated Relative Entalpies (ΔH_0) and Gibbs Free Energies (ΔG_{298}) for the Tautomers and Rotamers of the Structures Shown in Figure 1 (kcal mol^{-1}) in the Gas Phase

computational level	A	B	C	A$_1$	B$_1$
		ΔH_0			
MP2/6-31G(d,p)	0.19	0.00	2.07	6.54	2.49
CCSD(T)/6-31G(d,p)^a	0.99	0.00	2.18	7.22	2.40
MP2/6-31+G(d,p)	0.00	0.15	0.55	6.11	2.26
CCSD(T)/6-31+G(d,p)^b	0.46	0.00	0.52	0.52	2.15
MP2/6-31++G	6.60	6.41	0.00	11.08	7.41
CCSD(T)/6-31++G^c	4.57	3.43	0.00	8.96	4.66
		ΔG_{298}			
MP2/6-31G(d,p)	0.54	0.00	0.70	6.62	2.56
CCSD(T)/6-31G(d,p)^a	1.26	0.00	0.81	7.30	2.64
MP2/6-31+G(d,p)	1.15	1.51	0.00	7.31	3.33
CCSD(T)/6-31+G(d,p)^b	1.64	1.39	0.00	7.75	3.25
MP2/6-31++G	8.31	7.98	0.00	12.26	8.59
CCSD(T)/6-31++G^c	6.29	5.00	0.00	10.50	5.84

^{a} Single-point calculation using MP2/6-31G(d,p) optimized geometry. ^{b} Single-point calculation using MP2/6-31+G(d,p) optimized geometry. ^{c} Single-point calculation using MP2/6-31++G optimized geometry.
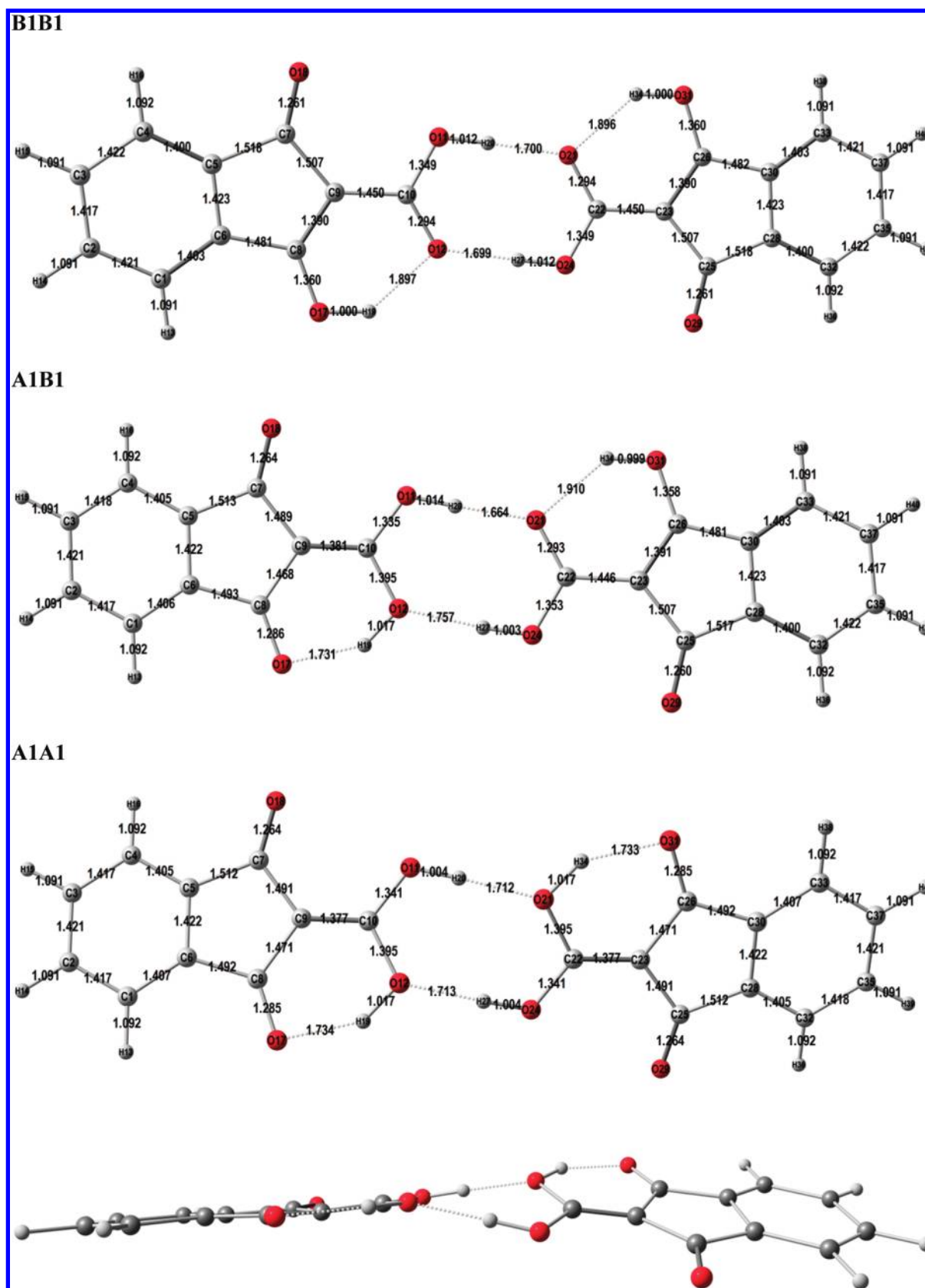
It should be noted that the optimizations of **A1B1** and **A1A1** dimers at the MP2 and DFT level using the Dunning (cc-pVTZ) basis set and the Pople basis set including polarization functions (6-31G(d,p)) predict too long of an OH bond (1.04−1.06 Å) when there is a such interaction (see last column in Table 3, Figure 3). Inclusion only of diffuse basis functions in the 6-31G basis set improves the results. Diffuse basis functions are spherical harmonics times Gaussian functions with small exponents. These functions have long tails that allow the electrons to be farther from the nuclei. This is especially important for calculations of systems that require a good description of electrons in weakly bound orbitals, i.e., description of noncovalent interactions such as hydrogen bonding. As a whole the MP2/6-31++G optimization gives correctly the bond lengths in the dimeric structures (Table 3). The optimized structures of the three dimers are presented in Figure 3.

The dimers could interconvert via intramolecular proton transfer (within one of the tautomeric forms constituting the dimers). The activation barrier of intramolecular proton transfer of **B1B1** → **A1B1** is calculated to be 5.82 kcal mol^{-1} for the forward reaction (Table 2) and 2.72 kcal mol^{-1} for the reverse reaction. The rate constant of the tautomerisation reaction, calculated by the Eyring equation, is found to be 3.36×10^8 s^{-1} for the forward and 6.30×10^{10} s^{-1} for the reverse reaction. This suggests that the proton transfer reaction is fast. Structural parameters for the transition state are given in Figure 4. Substantial changes are observed in the moiety in which the proton transfer occurs. The C8−C9 and C10−O12 bond lengths increase while the C9−C10 and C8−O17 bond lengths decrease in comparison with those of tautomer **B1** in dimer **B1B1**. The migrating proton is located approximately centrally between the O12 and O17 atoms.

3.2.1. NMR Spectrum. The ^{13}C CPMAS spectrum of 2-carboxyindan-1,3-dione recorded at a rotation speed of 10 kHz contains more resonances than the number of carbons in this
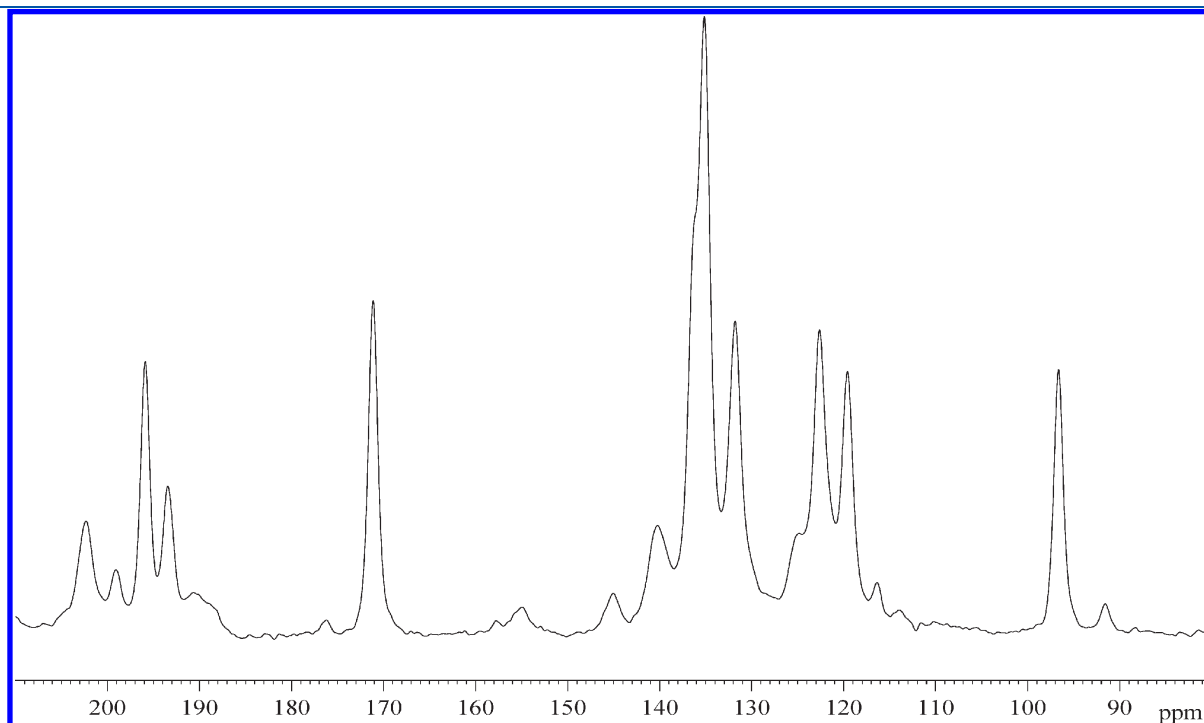
Figure 2. Solid-state NMR spectrum of 2-carboxyindan-1,3-dione recorded with rotation speed 10 kHz.

2028

dx.doi.org/10.1021/jp1100973 |*J. Phys. Chem. A* 2011, 115, 2026−2034

Figure 3. Dimeric structures of 2-carboxyindan-1,3-dione optimized at the MP2/6-31++G level. For dimer **A1A1** two projections are presented. Interatomic distances are in Å.

molecule, but some resonances are with low intensities. In order to identify the sidebands, spectra with two different rotation speeds were recorded. A rotation speed of ca. 8−10 kHz is too small to average fully the anisotropy of C=O, and sidebands are present on both sides of carbonyl resonances (Figure S1).

Table 2. Calculated Relative Entalpies (ΔH_0) and Gibbs Free Energies (ΔG_{298}) for the Dimeric Structures Shown in Figure 3 and Activation Barrier of the Proton Transfer Reaction B1B1 → A1B1 (kcal mol^{-1})^a

computational level	B1B1	B1A1	A1A1	TS(B1B1 → B1A1)	$\nu^{\#}$
		ΔH_0			
HF/6-31G(d,p)	0.00	0.02	9.14	2.21	1543.32i
HF/6-31+G(d,p)	0.00	6.51	14.93	8.47	1559.38i
HF/6-31++G	0.00	5.27	12.12	8.66	1663.84i
X3LYP/cc-pVTZ	0.00	5.01	10.12		
X3LYP/cc-pVTZ-	0.00	5.04	10.00		
MP2/6-31G(d,p)	0.00	5.88	12.66		
MP2/cc-pVTZ-	0.00	5.46	11.54		
MP2/6-31++G	0.00	4.63	9.27	5.55	1318.52i
		ΔG_{298}			
HF/6-31G(d,p)	3.31	0.00	9.12	3.43	1543.32i
HF/6-31+G(d,p)	0.00	6.08	13.96	8.69	1559.38i
HF/6-31++G	0.00	5.13	11.75	9.03	1663.84i
X3LYP/cc-pVTZ	0.00	4.16	9.52		
X3LYP/cc-pVTZ-	0.00	4.22	9.38		
MP2/6-31G(d,p)	0.00	5.34	13.26		
MP2/cc-pVTZ-	0.00	4.65	11.15		
MP2/6-31++G	0.00	3.10	9.68	5.82	1318.52i

^{a} Imaginary frequencies are in cm^{-1}.

However, the spectral region of 95−205 ppm is sideband free. The less intense resonances do not move upon increasing rotational speed, indicating that they originate from different molecular structures present in the sample.

The experimentally observed ^{13}C CPMAS spectrum of 2-carboxyindane-1,3-dione was examined for the existence of dimeric structures indicated by the quantum-chemical calculations. The GIAO OLYP/6-311+G(d,p) calculated carbon chemical shifts are compared to the solid-state ^{13}C chemical shifts (Table 4). The presence of structure **B1** as a part of **A1B1** or **B1B1**, and **A1** as a part of **A1B1**, is consistently reproduced at this level of calculation and agrees reasonably with reported experimental data (corroborates the existence of both dimeric structures in the solid state). The sets of chemical shifts for the two structural units **B1** and **A1** are well differentiable. For example, the observed difference between the C9 atoms in **B1** and **A1** is 4.8 ppm and the predicted one is 2.0−2.1 ppm; for C5 the experimental value is 5.5 ppm and the predicted one is 6.4−6.8 ppm; for C7 the experimental value is 2.4 ppm and the predicted one is 1.7−1.8 ppm.

3.2.2. IR Spectra. To confirm the existence of dimers **B1B1** and **A1B1** in the solid state, the IR spectra of 2-carboxyindan-1,3-dione were recorded by ATR and PE techniques. The obtained experimental frequencies were compared with the theoretically predicted ones (Table 5).

Similar to those of salicylic acid,[26] the IR spectra of 2-carboxylindan-1,3-dione show a complex behavior of a hydrogen-bonded dimer in the OH frequency region. The dimers in question contain two intramolecular and two intermolecular hydrogen bonds (Figure 3). The presence of two stable dimers complicates the interplay of these four different vibrational couplings of H-bonded network. Below we interpret qualitatively the spectral characteristics of 2-carboxylindan-1,3-dione in three frequency regions: O−H stretching (3600−3100 cm^{-1}), C=O

Table 3. Selected Interatomic Distances (Å) in Dimeric Structures B1B1, A1B1, and A1A1 (Figure 3) Obtained at Different Computational Levels

| computation level				distances				
	C10−O11	O11−H20	C10−O12	C8−O17	O17−H19	H20...O21	O12...H27	O12...H19
				Dimer **B1B1**				
MP2/6-31++G	1.349	1.012	1.294	1.360	1.000	1.700	1.699	1.897
MP2/6-31G(d,p)	1.317	0.996	1.261	1.323	0.990	1.688	1.688	1.789
MP2/cc-pVTZ-	1.313	0.995	1.256	1.318	0.990	1.762	1.762	1.757
X3LYP/cc-pVTZ-	1.308	0.998	1.256	1.309	0.994	1.664	1.664	1.734
X3LYP/cc-pVTZ	1.306	0.998	1.255	1.307	0.994	1.661	1.661	1.737
				Dimer **A1B1**				
MP2/6-31++G	1.335	1.014	1.395	1.286	1.731	1.664	1.757	1.017
MP2/6-31G(d,p)	1.306	0.996	1.335	1.259	1.507	1.670	1.818	1.041
MP2/cc-pVTZ-	1.301	0.995	1.331	1.253	1.512	1.655	1.796	1.037
X3LYP/cc-pVTZ-	1.296	1.000	1.326	1.248	1.493	1.642	1.808	1.046
X3LYP/cc-pVTZ	1.294	1.000	1.326	1.245	1.505	1.637	1.807	1.042
				Dimer **A1A1**				
MP2/6-31++G	1.341	1.004	1.395	1.285	1.734	1.712	1.713	1.017
MP2/6-31G(d,p)	1.312	0.983	1.334	1.259	1.496	1.796	1.797	1.045
MP2/cc-pVTZ-	1.308	0.981	1.330	1.252	1.499	1.776	1.776	1.042
X3LYP/cc-pVTZ-	1.304	0.983	1.323	1.249	1.459	1.781	1.781	1.059
X3LYP/cc-pVTZ	1.302	0.983	1.323	1.246	1.475	1.778	1.778	1.053
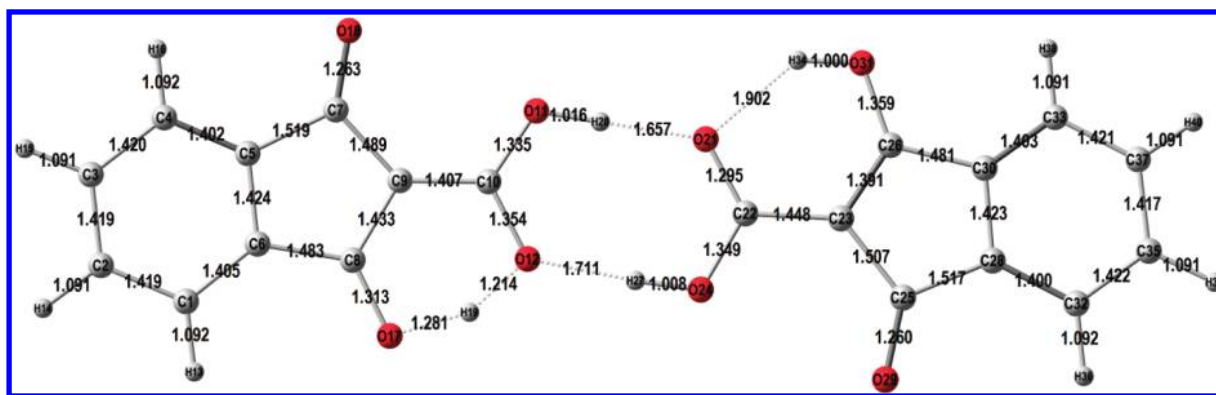
Figure 4. Transition state **B1B1** → **A1B1** located at the MP2/6-31++G level. Interatomic distances are in Å.

Table 4. Experimental (Figure 2) and GIAO Calculated ^{13}C Chemical Shifts of Tautomers A1 and B1 for 2-Carboxyindane-1,3-dione in Dimers B1B1 and A1B1 (Figure 3) Optimized at the MP2/6-31++G level

	exptl		OLYP/6-311+G(d,p)		
	B1[a]	A1[a]	B1 (B1B1)	B1 (A1B1)	A1 (A1B1)
C1	119.3	122.3	120.9	124.0	122.6
C2	131.5	135.0	132.9	133.1	133.1
C3	135.0	140.2	135.5	136.1	135.3
C4	122.3	124.9	123.5	121.9	123.1
C5	134.7	140.2	132.2	132.6	139.0
C6	136.0	144.7	136.4	136.3	137.6
C7	195.5	193.1	191.4	191.3	189.6
C8	199.0	202.5	188.8	189.2	198.3
C9	96.4	91.6	101.7	100.8	98.7
C10	170.8	170.8	175.8	175.3	170.5

[a] Tautomer in dimeric structure.

Table 5. Selected MP2/6-31++G Calculated and Experimental (Figure 5) Infrared Frequencies IR in Dimers B1B1 and A1B1[a]

calculated		experimental		
A1B1	B1B1	A1B1	B1B1	assignment
		O−H Frequency Region		
3548 (142)		3545 w		$\nu(OH)_{ind}$ (**B1**)
	3533 (80)		3537 m	$\nu_s(OH)_{ind}$ (**B1**), degenerate
3478 (2779)		3521 m		$\nu_s(OH)_{carboxy}$ (inter) + $\nu(OH)_{ind}$ (intra)
	3330 (5945)		3346 m	$\nu_s(OH)_{carboxy}$ (inter) + $\nu_{as}(C-C)$
3215 (3608)		3281 m		$\nu_{as}(OH)_{carboxy}$ + $\nu(OH)_{ind}$ (intra)
	3228 (0.02)			$\nu_{as}(OH)_{carboxy}$ + $\nu(OH)_{ind}$ (intra)
		C=O Frequency Region		
1787 (1289)				$\nu_s(C=O)_{ind}$ (**A1**) + $\nu(C=C)_{ind}$ (**A1**) + $\delta(OH)_{carboxy}$ (inter)
	1701 (514)		1698 s	$\nu_s(C=O)$ + $\nu_s(C-C)$ + $\delta_s(OH)_{carboxy}$
1701 (573)				$\nu(C=C)_{ind}$ (**B1**) + $\nu(C-C)$ (**B1**) + $\delta(OH)_{carboxy}$ (inter)
	1661 (477)		1667 m	$\nu_{as}(C=C)_{ind}$ + $\nu_s(C=O)$ + $\nu_s(C-C)$
1665 (482)				$\nu_s(C=O)$ (**A1**) + $\delta_s(OH)$ (**A1**) + $\delta(OH)_{carboxy}$ (inter)
	1644 (1821)		1640 m	$\nu(C=C)_{ind}$ + $\nu_{as}(C-C)$ + $\delta(OH)_{carboxy}$ (inter)
1649 (922)				$\nu(C=C)_{ind}$
		Low-Frequency Region		
	385 (0.04)			$\nu(OH...O)_{inter}$ + $\nu_s(C-C)$ (**B1**)
368 (4)			370 m	$\nu(OH...O)_{intra}$ (**A1**) + $\nu(OH...O)_{inter}$
	324 (14)		300 w	$\delta_s(OH...O)_{ind}$ (**B1**) + δ (OH...O)$_{inter}$

2031

dx.doi.org/10.1021/jp1100973 |*J. Phys. Chem. A* 2011, 115, 2026–2034

Table 5. Continued

calculated		experimental		
A1B1	B1B1	A1B1	B1B1	assignment
327 (7)				$\delta(OH..O)_{ind}$ (B1) + $\nu(OH...O)_{inter}$ + $\delta(C=O)_{ind}$ (B1)
	257 (20)		255 s	$\delta_{as}(OH...O)_{ind}$ (B1) + $\delta(OH...O)_{inter}$ + $\delta_{as}(C-C)$ (B1)
258 (9)				$\delta(OH...O)_{ind}$ (B1) + $\nu(OH...O)_{inter}$
	209 (28)		203 s	$\delta (OH...O)_{inter}$
208 (19)				$\delta (OH...O)_{inter}$

^{a} Frequencies, ν, are in cm^{-1} and intensities, I (in parentheses), in km mol^{-1}. The scale factors used are 1.064 for vibrational frequencies in the region 3600−3100 cm^{-1} and 1.03 for the region 1800−1500 cm^{-1}, and without scale factor for the low-frequency vibrations (below 400 cm^{-1}). Notation: ν_s, symmetric stretching vibration; ν_{as}, antisymmetric stretching vibration; δ, bending vibration; δ_s, symmetric bending vibration; inter, intermolecular hydrogen bond; intra, intramolecular hydrogen bond; ind, indandione unit; carboxy, carboxy group in the indandione unit.
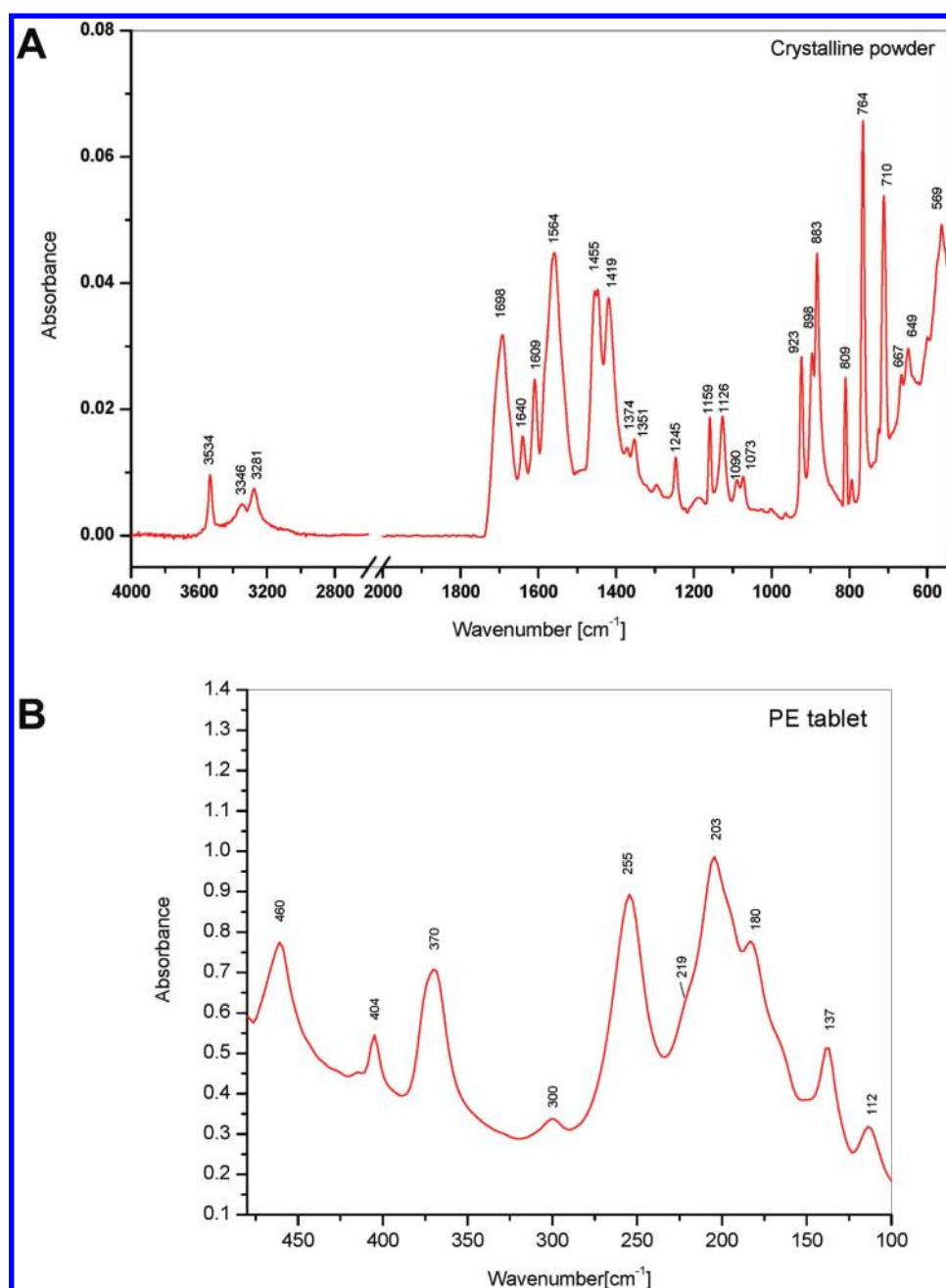

Figure 5. Solid-state IR spectrum of 2-carboxyindan-1,3-dione in crystalline powder (A) and in PE tablet (B).

2032

dx.doi.org/10.1021/jp1100973 |J. Phys. Chem. A 2011, 115, 2026–2034

stretching (1720−1550 cm^{-1}), and low frequency (400−100 cm^{-1}).

O−H Frequency Region. A indication for the presence of dimer **A1B1** in solid phase can be obtained by the line shape of the ν_{OH} band at 3534 cm^{-1} (Figure 5A), which seems not to be a single one. After application of Fourier deconvolution of the IR spectrum in this region, it is revealed that this band is split into three components: 3545, 3537, and 3521 cm^{-1}. These bands of the multiplet at 3534 cm^{-1} can be assigned as stretching vibrations of the OH group connected to the five-membered ring of indandione. Their high frequencies suggest a weak intramolecular H-bond between this OH group and the acid carbonyl group. In support of this are the optimized geometries of dimers **A1B1** and **B1B1** (Figure 3), as well as the calculated frequencies (Table 4), whose shape modes correspond to the high-frequency modes of the OH group.

The experimental bands at 3346 and 3281 cm^{-1} can be assigned to symmetric and antisymmetric O−H stretching vibrations related to the dimer hydrogen bonds of **B1B1** (Figure 3). The intermolecular hydrogen bonds forming a dimer are much stronger than the weak intramolecular hydrogen bonds associated with high-frequency modes at 3534 cm^{-1}.

During tautomeric transformation of the **B1B1** acid carbonyl group into the OH group of **A1B1**, a new ν_{OH} band should appear (near the predicted one) at 3521 cm^{-1}, while the stretching vibrational mode of the OH group connected to the indandione five-membered ring is predicted at 3548 cm^{-1}. This band is revealed at 3545 cm^{-1} in the experimental IR spectrum after resolution enhancement (by Fourier deconvolution) of the multiplet band at 3534 cm^{-1}.

C=O Frequency Region. Two carbonyl bands at 1713 and 1746 cm^{-1} are usually observed in the IR spectra of indandiones that correspond to asymmetric ν_{as}(C=O) and symmetric ν_s-(C=O) vibrations.[27] However, in the case of 2-carboxylindan-1,3-dione (enol form stabilized by H-bond), two frequency bands are observed for the ν(C=O) and ν(C=C) stretching vibrations at 1698 and 1640 cm^{-1}, respectively. This fact confirms the presence of dimer **BB** in solid phase. However, a theoretically predicted high-intensity C=O band of dimer **A1B1** at 1787 cm^{-1} (Table 4) cannot be observed in the experimental IR spectrum, which supposes a small amount of this form in the solid mixture.

Low-Frequency Region. In the far-infrared spectrum of 2-carboxylindan-1,3-dione are observed several in-plane and out of-plane low-frequency vibrations below 400 cm^{-1} (Figure 5B). The most interesting ones are collective inter- and intramolecular OH...O stretching vibrations which have different frequencies for dimers **B1B1** and **A1B1** (Table 4). Coupled inter-intramolecular vibrations of hydrogen-bonded network can be assigned at 300 and 255 cm^{-1}, while bending modes of the hydrogen bonds appear at 203 cm^{-1}. The corresponding low-frequency modes predicted at the MP2/6-31++G level for dimers **A1B1** and **B1B1** are close and cannot be used for dimer identificaton (Table 4). The quantum-chemical calculations predict that the mode involving only intermolecular hydrogen bond stretchings should be observed below 100 cm^{-1}.

4. CONCLUSIONS

A rare case of solid-state tautomerism is reported. 2-Carboxyindane-1,3-dione contains two tautomers forming a hydrogen-bonded dimer. The detailed description is based on the

quantum-chemical calculations and experimental ^{13}C NMR shifts as a more reliable source of information than IR spectroscopy, due to the complexity of the vibrational modes of the compound. The applied combined approach (quantum-chemical calculations, ^{13}C CPMAS NMR, and IR) demonstrates its potential as an alternative way to determine the solid-state structure of a compound when no single crystals can be obtained.

■ ASSOCIATED CONTENT

S **Supporting Information.** Spectra of 2-carboxyindane-1,3-dione recorded with two different rotation speeds. This material is available free of charge via the Internet at http://pubs.acs.org.

■ AUTHOR INFORMATION

Corresponding Author
*E-mail venelin@orgchm.bas.bg; fax ++359 2 8700225.

■ ACKNOWLEDGMENT

■ REFERENCES

(1) (a) Hansen, P. E.; Rozwadowski, Z.; Dziembowska, T. *Curr. Org. Chem.* **2009**, *13*, 194–215. (b) Bertolasi, V.; Gilli, P.; Gilli, G. *Curr. Org. Chem.* **2009**, *13*, 250–268. (c) Hadjoudis, E.; Chatziefhtimou, S. D.; Mavridis, I. M. *Curr. Org. Chem.* **2009**, *13*, 269–286. (d) Hadjoudis, E. *Mol. Engin.* **1995**, *5*, 301–337.

(2) (a) Guo, J.; Liu, L.; Jia, D.; Liu, G. *Struct. Chem.* **2009**, *20*, 393–398. (b) Zhang, T.; Liu, G.; Liu, L.; Jia, D.; Zhang, L. *Chem. Phys. Lett.* **2006**, *427*, 443–448. (c) Peng, B.-H.; Liu, G.-F.; Liu, L.; Jia, D.-Z.; Yu, K.-B. *J. Photochem. Photobiol., A* **2005**, *171*, 243–249. (d) Peng, B.-H.; Liu, G.-F.; Liu, L.; Jia, D.-H. *Tetrahedron* **2005**, *61*, 5926–5932. (e) Sliwa, M.; Letard, S.; Malfani, I.; Nierlich, M.; Lacroix, P. G.; Asahi, T.; Masuhara, H.; Yu, P.; Nakatani, K. *Chem. Mater.* **2005**, *17*, 4727–4735.

(3) (a) Takeda, S.; Chihara, H.; Inabe, T.; Mitani, T.; Maruyama, Y. *Mol. Cryst. Liq. Cryst.* **1992**, *216*, 235–240. (b) Takeda, S.; Chihara, H.; Inabe, T.; Mitani, T.; Maruyama, Y. *Chem. Phys. Lett.* **1992**, *189*, 13–17.

(4) (a) Inabe, T.; Luneau, I.; Mitani, T.; Maruyama, Y.; Takeda, S. *Bull. Chem. Soc. Jpn.* **1994**, *67*, 612–621. (b) Inabe, T.; Hoshino-Miyajima, N.; Luneau, I.; Mitani, T.; Murayama, Y. *Bull. Chem. Soc. Jpn.* **1994**, *67*, 622–632. (c) Takeda, S.; Inabe, T.; Benedict, C.; Langer, U.; Limbach, H. H. *Ber. Bunsenges. Phys. Chem.* **1998**, *102*, 1358–1369.

(5) (a) Alarcon, S. H.; Olivieri, A. C.; Nordon, A.; Harris, R. K. *J. Chem. Soc., Perkin Trans. 2* **1996**, 2293–2296.

(6) (a) Pizzala, H.; Carles, M.; Stone, W. E. E.; Thevand, A. *J. Chem. Soc., Perkin Trans. 2* **2000**, 935–939. (b) Pizzala, H.; Carles, M.; Stone, W. E. E.; Thevand, A. *J. Mol. Struct.* **2000**, *526*, 261–268.

(7) del Amo, J. M. L.; Langer, U.; Torres, V.; Buntkowsky, G.; Vieth, H.-M.; Perez-Torralba, M.; Sanz, D.; Claramunt, R. M.; Elguero, J.; Limbach, H.-H. *J. Am. Chem. Soc.* **2008**, *130*, 8620–8632.

(8) Perez-Torralba, M.; Lopez, C.; Perez-Medina, C.; Claramunt, R. M.; Pinilla, E.; Torres, M. R.; Alkorta, I.; Elguero *J. Cryst. Eng. Commun.* **2010**, *12*, 4052–4055.

(9) Enchev, V.; Abrahams, I.; Angelova, S.; Ivanova, G *J. Mol. Struct. Theochem* **2005**, *719*, 169–175.

(10) Michael, A.; Gabriel, S. *Berichte* **1877**, *10*, 391–393.

(11) Gabriel, S.; Neumann, A. *Berichte* **1893**, *26*, 951–955.

(12) Tirzîtis, G.; Žagats, R.; Vanags, G. *Latvijas PRS Zinatnu Acad. Vestus* **1962**, 97–101.

(13) Angelova, S.; Enchev, V.; Kostova, K.; Rogojerov, M.; Ivanova, G. *J. Phys. Chem. A* **2007**, *111*, 9901–9913.

(14) (a) Bechtel, F.; Gaultier, J.; Hauw, C. *Cryst. Struct. Commun.* **1973**, *3*, 469–472. (b) Halcrow, M. A.; Powell, H. R.; Duer, M. J. *Acta Crystallogr., Sect. B* **1996**, *52*, 746–752. (c) Foces-Foces, C.; Fontenas, C.; Elguero, J.; Sobrados, I. *An. Quim. Int. Ed.* **1997**, *93*, 219–224. (d) Kubicki, M. *Acta Crystallogr., Sect. B* **2004**, *60*, 191–196. (e) Song, J.; Mishima, M.; Rappoport, Z. *Org. Lett.* **2007**, *9*, 4307–4310. (f) Chierotti, M. R.; Ferrero, L.; Garino, N.; Gobetto, R.; Pellegrino, L.; Braga, D.; Grepioni, F.; Maini, L. *Chem.—Eur. J.* **2010**, *16*, 4347–4358.

(15) Gonzales, C.; Schlegel, H. B. *J. Chem. Phys.* **1989**, *90*, 2154–2161.

(16) (a) Piecuch, P.; Kucharski, S. A.; Kowalski, K.; Musail, M. *Comput. Phys. Commun.* **2002**, *149*, 71–96. (b) Bentz, J. L.; Olson, R. M.; Gordon, M. S.; Schmidt, M. W.; Kendall, R. A. *Comput. Phys. Commun.* **2007**, *176*, 589–600. (c) Olson, R. M.; Bentz, J. L.; Kendall, R. A.; Schmidt, M. W.; Gordon, M. S. *J. Comput. Theor. Chem.* **2007**, *3*, 1312–1328.

(17) Schmidt, M. W.; Baldridge, K. K.; Boatz, J. A.; Elbert, S. T.; Gordon, M. S.; Jensen, J. H.; Koseki, S.; Matsunaga, N.; Nguyen, K. A.; Su, S.; Windus, T. L.; Dupuis, M.; Montgomery, J. A. *J. Comput. Chem.* **1993**, *14*, 1347–1363.

(18) Granovsky, A. A. Firefly ver. 7.1.G, http://classic.chem.msu.su/gran/firefly/index.html.

(19) Xu, X.; Goddard, W. A. *Proc. Natl. Acad. Sci. U.S.A.* **2004**, *101*, 2673–2677.

(20) Granovsky, A. A. Private communication, 2009, http://classic.chem.msu.su/cgi-bin/ceilidh.exe/gran/gamess/forum/?C3c360e4ddT5P-7293-844+00.htm.

(21) Scott, A. P.; Radom, L. *J. Phys. Chem.* **1996**, *100*, 16502–16513.

(22) Andersson, M. P.; Uvdal, P. *J. Phys. Chem. A* **2005**, *109*, 2937–2941.

(23) (a) Ditchfield, R. *Mol. Phys.* **1974**, *27*, 789–807. (b) Wolinski, K.; Hilton, J. F.; Pulay, P. *J. Am. Chem. Soc.* **1990**, *112*, 8251–8260.

(24) Frisch, M. J.; Trucks, G. W.; Schlegel, H. B.; Scuseria, G. E.; Robb, M. A.; Cheeseman, J. R.; Montgomery, J. A., Jr.; Vreven, T.; Kudin, K. N.; Burant, J. C.; Millam, J. M.; Iyengar, S. S.; Tomasi, J.; Barone, V.; Mennucci, B.; Cossi, M.; Scalmani, G.; Rega, N.; Petersson, G. A.; Nakatsuji, H.; Hada, M.; Ehara, M.; Toyota, K.; Fukuda, R.; Hasegawa, J.; Ishida, M.; Nakajima, T.; Honda, Y.; Kitao, O.; Nakai, H. ; Klene, M.; Li, X.; Knox, J. E.; Hratchian, H. P.; Cross, J. B.; Adamo, C.; Jaramillo, J.; Gomperts, R.; Stratmann, R. E.; Yazyev, O.; Austin, A. J.; Cammi, R.; Pomelli, C.; Ochterski, J. W.; Ayala, P. Y.; Morokuma, K.; Voth, G. A.; Salvador, P.; Dannenberg, J. J.; Zakrzewski, V. G.; Dapprich, S.; Daniels, A. D.; Strain, M. C.; Farkas, O.; Malick, D. K.; Rabuck, A. D.; Raghavachari, K.; Foresman, J. B.; Ortiz, J. V.; Cui, Q.; Baboul, A. G.; Clifford, S.; Cioslowski, J.; Stefanov, B. B.; Liu, G.; Liashenko, A.; Piskorz, P.; Komaromi, I.; Martin, R. L.; Fox, D. J.; Keith, T.; Al-Laham, M. A.; Peng, C. Y.; Nanayakkara, A.; Challacombe, M.; Gill, P. M. W.; Johnson, B.; Chen, W.; Wong, M. W.; Gonzalez, C. Pople, J. A. *Gaussian 03*, revision B.04; Gaussian, Inc.: Pittsburgh PA, 2003.

(25) Gavezzotti, A. *Acta Crystallogr., Sect. B* **2008**, *64*, 401–403.

(26) (a) Dunn, G. E.; McDonald, R. S. *Can. J. Chem.* **1969**, *47*, 4577–4588. (b) Boczar, M.; Boda, Ł.; Wójcik, M. J. *J. Chem. Phys.* **2006**, *124*, 084306. (c) Wójcik, M. J.; Boda, Ł. *J. Mol. Struct.* **2006**, *844−845*, 3–12.

(27) Sigalov, M.; Gabriel Lemcoff, N.; Shainyan, B.; Chipanina, N.; Aksamentova, T. *Eur. J. Org. Chem.* **2010**, 2800–2811.